Supplementary Material

Transmural heterogeneity of cellular level power output is reduced in human heart failure

Premi Haynes, MS[1, 2], Kristofer E. Nava, BS[1, 2], Benjamin A. Lawson, BS[1, 2], Charles S. Chung, PhD[1, 2], Mihail I. Mitov, PhD[1,2], Stuart G. Campbell, PhD[1,2], Arnold J. Stromberg, PhD[3], Sakthivel Sadayappan, PhD[4], Mark R. Bonnell, MD[5], Charles W. Hoopes, MD[5], Kenneth S. Campbell, PhD[1, 2]

[1]Department of Physiology and [2]Center for Muscle Biology, University of Kentucky, Lexington, KY, [3]Department of Statistics, University of Kentucky, Lexington, KY, [4]Department of Cell and Molecular Physiology, Stritch School of Medicine, Loyola University, Chicago, [5]Division of Cardiothoracic Surgery, University of Kentucky, Lexington, KY.

Methods

Functional Assays

Chemically Permeabilized Multicellular Preparations

Multicellular cardiac preparations were obtained as previously described for rat samples [1]. Frozen tissue specimens (~5 x 5 x 5 mm) were placed in 10 ml of relaxing solution (see Solutions), mechanically disrupted using a tissue homogenizer (Polytron, Brinkman Instruments, Westbury, NY), and chemically permeabilized using Triton X-100 (30 min, 1% v/v). The permeabilized samples were stored in relaxing solution at 4°C for up to 12 hours before use. Jweied *et al.* showed that previously frozen and fresh tissue samples yield comparable data with these techniques [2].

Mechanical Experiments

Individual preparations (Figure S1) were attached between a force transducer (resonant frequency 600 Hz, model 403, Aurora Scientific, Aurora, Ontario, Canada) and a motor (step time 0.6 ms, model 312B, Aurora) by crimping their ends into metal troughs (shaped from 27 gauge tubing) with overlays of 4-0 nylon monofilament. This technique is illustrated in Figure 1B of Campbell & Moss [3]. The experimental temperature was 15°C.

The samples were stretched in pCa 9.0 solution (see Solutions) by manually adjusting the manipulator holding the motor until the mean sarcomere length of the preparation (measured by video microscopy) was within 1% of 2.20 μm. Cross-sectional area ($2.17 \pm 0.07 \times 10^{-8}$ m^2) was estimated from the video images by assuming that each

preparation had a circular profile. The average length of the preparations once sarcomere length had been set was 688 ± 11 μm. If it is assumed that single human myocytes [4] have average dimensions of 100 x 25 x 25 μm, and that the relative collagen content of the preparations ranged from 5 to 58%, each myocardial preparation probably contained between 13 and 30 single myocytes.

Each preparation was initially immersed in pCa 4.5 solution to maximally activate the sample. Once tension had attained steady-state, the muscle was subjected to 3 'saw-tooth' lengthening/shortening perturbations to assess muscle stiffness (magnitude 0.04 l_0, velocity ±0.12 l_0 s^{-1}, inter-perturbation interval 100 ms, where l_0 is the muscle length) and a rapid shortening/re-stretch maneuver (0.2 l_0, 20 ms duration) before being returned to pCa 9.0 solution. Similar trials were subsequently performed for each preparation using solutions with pCa values ranging from 9.0 to 5.0. The isometric force values measured in the trials were used to generate tension-pCa curves (Figure 3, main text) by fitting the raw data to an equation of the form

$$y = A + B\frac{\left[Ca^{2+}\right]^n}{\left[Ca^{2+}\right]^n + \left[Ca_{50}^{2+}\right]^n} \qquad (1)$$

where A corresponds to passive force, B represents Ca^{2+} activated force, n is the Hill coefficient, and $\left[Ca_{50}^{2+}\right]$ is the free Ca^{2+} concentration required to develop half the maximum Ca^{2+}-dependent force.

Once the measurements at intermediate Ca^{2+} levels were complete, the preparation was re-activated in the pCa 4.5 solution. After force had reached the steady-state for

this condition, a sequence of trials was initiated in which the preparation was allowed to shorten for 75 ms against a variety of pre-set loads (Figure S13).This technique was used to establish the preparation's force velocity curve. Shortening velocity was determined for each trial from the slope of a regression line fitted to the final 50 ms of the force clamp [5]. The average r^2 value for these lines was 0.991 which indicates that the velocity of interfilamentary movement was not markedly dependent on the total distance shortened [6, 7].

A hyperbolic curve was fitted to the force-velocity data using Hill's equation

$$(F + a) \cdot (V + b) = (F_0 + a) \cdot b \qquad (2)$$

where F is the force at shortening velocity V, and F_0 is the maximum isometric force [8]. The constants a and b have dimensions of force and velocity respectively. Power values were calculated as the product of force and velocity (Figure 1A, main text).

The inclusion criteria accepted all preparations that developed an active force that varied systematically with Ca^{2+}. Run-down (calculated as the reduction in force measured during activations in pCa 4.5 solution at the beginning and end of mechanical tests) was 7.6 ± 1.2 % (n=141 preparations). The r^2 value for the tension-pCa curves was 0.976 ± 0.002.

Passive tension was 7.6 ± 0.4% of maximum active tension (n=141 preparations) and did not correlate with either maximum active tension or maximum power.

All mechanical tests were performed using SLControl software [9]. Curve-fitting and data analysis were performed using custom software written in MATLAB (Mathworks,

Natick, MA). Permeabilized samples that were not used for functional tests were saved for subsequent biochemical assays.

Solutions

The relaxing solution used for isolating the myocardial preparations contained (in mmol L^{-1}): 100 KCl, 10 imidazole, 4 ATP, 2 EGTA and 5 $MgCl_2$ and two protease inhibitors (phenylmethylsulfonide 500 µmol L^{-1} and leupeption 40 µmol L^{-1}). All pCa (= $-\log_{10}[Ca^{2+}]$) solutions contained (in mmol L^{-1}): 20 imidazole, 14.5 creatine phosphate, 7 EGTA, 4 MgATP, 1 free Mg^{2+}, free Ca^{2+} ranging from 1 nmol L^{-1} (pCa 9.0) to 32 µmol L^{-1} (pCa 4.5) and sufficient KCl to adjust the ionic strength to 180 mmol L^{-1}. The precise composition of each pCa solution was determined using Maxchelator software (version 2.50) and NIST stability constants [10].

Biochemical Assays

SDS-PAGE Gels

The relative content (Tables S1 and S2) and phosphorylation status (Table S3) of key sarcomeric proteins were examined using gel electrophoresis. Some posttranslational modifications are thought to be regulated on a beat to beat basis in living myocardium and may thus be sensitive to the precise experimental conditions [11]. However, the biochemical data reported here should be representative of the preparations that were analyzed in the functional measurements. This is because the biochemical assays were performed using chemically permeabilized specimens that had been prepared for functional testing but which were not, in the event, used for that purpose.

Samples were initially homogenized in a urea-thiourea sample buffer (in mol L^{-1}, 8 Urea, 2 Thiourea, 0.075 M DTT, and 0.05 Tris-HCl, with 3% SDS w/v, pH 6.8) [12]. Once homogenization was complete, the protein concentration in the sample was determined using a Lowry protein assay (RC/DC kit, Bio-Rad, Hercules, CA).

Precast polyacrylamide gels (Tris-HCl, 26 well, Bio-Rad, Hercules, CA) were loaded with samples containing 1 µg of protein. Each gel was run at 200 V for 55 minutes and then stained to assess phosphoproteins using Pro-Q Diamond stain (Invitrogen, Carlsbad, CA). After the gel had been scanned using a Typhoon Trio+ imager (GE Healthcare, Piscataway, NJ), the gel was re-stained with SYPRO Ruby (Invitrogen, Carlsbad, CA) to assess total protein content, and re-scanned.

The phosphorylation levels of selected proteins were calculated by integrating the densitometry profile (ImageQuant TL software, GE Healthcare) of each band in the Pro-Q stained image and dividing the result by the corresponding data calculated for the SYPRO Ruby stained image. Relative phosphorylation levels and relative protein contents were calculated by normalizing to data obtained for a non-failing sub-epicardial sample that was loaded onto every gel as a control [13].

The relative content of the N2B and N2BA isoforms of titin were assessed using a vertical agarose gel system [14]. The gel was cast using 1.2% w/v Sea Kem Gold Agarose, 30% v/v Glycerol, 0.05 M Tris-base, 0.384 M Glycine, and 0.1% w/v SDS. The samples (3 µL at a protein concentration of 1 µg μL^{-1}) were loaded on the gels and run at 4°C at a constant voltage of 40 V for the first 3hours, and then at 70 V for ~4 hours. Gels were stained with SYPRO Ruby and analyzed as described above. Relative

protein contents were calculated by normalizing to data obtained for a non-failing sub-endocardial sample that was loaded onto every gel as a control.

Western Blots

Immunoblotting was performed to assess the site-specific phosphorylation of cTnI and cMyBP-C. Experiments investigating the phosphorylation of cTnI at Ser23/24 were performed using commercially available antibodies [15] (PSer23/24, antibody # 4004, Cell Signaling Technologies, Danvers, MA; cTnI, sc-52266, Santa Cruz, Dallas, TX). The antibodies used to assess site-specific phosphorylation of cMyBP-C at Ser-273, Ser-282, and Ser-302 have been described by Govindan *et al* [16].

Samples (3 μL volume, at a protein concentration of 1 μg μL^{-1}) were run on 10% precast polyacrylamide gels (Mini-Protean TGX, 15 well, Bio-Rad) for 30 minutes at 200 V and then transferred onto polyvinylidene difluoride membranes. Each membrane was first incubated with the primary antibody (1:1000 dilution) and then with the fluorescent secondary antibody (anti-mouse DyLight 680 for cTnI, PSer23/24 cTnI, and cMyBP-C; anti-rabbit 800 for phosphorylated cMyBP-C, both antibodies from Cell Signaling Technologies) at a 1:7500 dilution. All bands were subsequently visualized using a LI-COR Odyssey imaging system (LI-COR Biosciences, Lincoln, NE) and analyzed using Odyssey V3.0 image analysis software.

The relative phosphorylation of the site was calculated by integrating the densitometry profiles for the phosphorylated protein and total protein bands, and normalizing to data for a single rabbit muscle sample (for phosphorylated and total cTnI) or a non-failing

sub-epicardial human sample (for phosphorylated and total cMyBP-C) that was loaded on to every gel as a control.

Histology

Tissue samples were transferred from long-term storage in the vapor phase of liquid nitrogen to a cryostat maintained at -26°C. Samples were placed in 10 x 10 x 5 mm cryomolds and covered with optimal cutting temperature (OCT) medium (Schaumburg, IL). Samples were then cut into 10 μm sections and air dried on glass slides for 1 hour at room temperature. A staining method similar to that described by Hanley *et al.* [17] was used. The slides were initially covered in Bouin's fixative solution and incubated at 56ºC for an hour. Next, the slides were rinsed in deionized water and placed for 2 hours in a 0.1% Sirius red solution (w/v) dissolved in 1.3% saturated picric acid. The slides were then washed with 0.5% acetic acid, dehydrated in 95% and 100% ethanol, and finally equilibrated in xylene [17]. Sections, which had an average cross-sectional area of ~16 mm^2, were imaged in bright field [18] with a 10x objective (Olympus BX61VS microscope) and analyzed using custom software written in MATLAB (The Mathworks, Natick, MA). A total of 150 images were analyzed in duplicate by observers who were blinded to the experimental groups and could not identify the patient/donor or the transmural sources of the samples.

Limitations of Using Human Tissue Samples

The mean age of the patients with heart failure was 49 (range 20 to 65) while that of the organ donors was 35 (range 18 to 59). Females donated 20% of the failing hearts and 50% of the non-failing organs. All of the organ donors had been treated in Intensive

Care Units before their hearts were harvested, and some may have had additional comorbidities such as diabetes and/or hypertension. Although this is a limitation, none of the donors had a prior history of ventricular dysfunction and their hearts are the best control organs that are available for this type of study.

References

[1] Mitov MI, Holbrook AM, Campbell KS. Myocardial short-range force responses increase with age in F344 rats. J Mol Cell Cardiol. 2009;46:39-46.

[2] Jweied EE, McKinney RD, Walker LA, Brodsky I, Geha AS, Massad MG, et al. Depressed cardiac myofilament function in human diabetes mellitus. Am J Physiol Heart Circ Physiol. 2005;289:H2478-83.

[3] Campbell KS, Moss RL. History-dependent mechanical properties of permeabilized rat soleus muscle fibers. Biophys J. 2002;82:929-43.

[4] Zafeiridis A, Jeevanandam V, Houser SR, Margulies KB. Regression of cellular hypertrophy after left ventricular assist device support. Circulation. 1998;98:656-62.

[5] Ford LE, Nakagawa K, Desper J, Seow CY. Effect of osmotic compression on the force-velocity properties of glycerinated rabbit skeletal muscle cells. The Journal of general physiology. 1991;97:73-88.

[6] Brenner B. The necessity of using two parameters to describe isotonic shortening velocity of muscle tissues: the effect of various interventions upon initial shortening velocity (vi) and curvature (b). Basic research in cardiology. 1986;81:54-69.

[7] Brenner B, Jacob R. Calcium activation and maximum unloaded shortening velocity. Investigation on glycerinated skeletal and heart muscle preparations. Basic research in cardiology. 1980;75:40-6.

[8] Hill AV. The heat of shortening and the dynamic constants of muscle. Proc R Soc Lond B Biol Sci. 1938;126:136-95.

[9] Campbell KS, Moss RL. SLControl: PC-based data acquisition and analysis for muscle mechanics. Am J Physiol Heart Circ Physiol. 2003;285:H2857-H64.

[10] Patton C, Thompson S, Epel D. Some precautions in using chelators to buffer metals in biological solutions. Cell Calcium. 2004;35:427-31.
[11] Monasky MM, Biesiadecki BJ, Janssen PM. Increased phosphorylation of tropomyosin, troponin I, and myosin light chain-2 after stretch in rabbit ventricular myocardium under physiological conditions. Journal of molecular and cellular cardiology. 2010;48:1023-8.
[12] Blough ER, Rennie ER, Zhang F, Reiser PJ. Enhanced electrophoretic separation and resolution of myosin heavy chains in mammalian and avian skeletal muscles. Anal Biochem. 1996;233:31-5.
[13] Campbell SG, Haynes P, Kelsey Snapp W, Nava KE, Campbell KS. Altered ventricular torsion and transmural patterns of myocyte relaxation precede heart failure in aging F344 rats. American journal of physiology Heart and circulatory physiology. 2013;305:H676-86.
[14] Warren CM, Krzesinski PR, Greaser ML. Vertical agarose gel electrophoresis and electroblotting of high-molecular-weight proteins. Electrophoresis. 2003;24:1695-702.
[15] Dong WJ, Jayasundar JJ, An J, Xing J, Cheung HC. Effects of PKA phosphorylation of cardiac troponin I and strong crossbridge on conformational transitions of the N-domain of cardiac troponin C in regulated thin filaments. Biochemistry. 2007;46:9752-61.
[16] Govindan S, McElligott A, Muthusamy S, Nair N, Barefield D, Martin JL, et al. Cardiac myosin binding protein-C is a potential diagnostic biomarker for myocardial infarction. Journal of molecular and cellular cardiology. 2012;52:154-64.

[17] Hanley PJ, Young AA, LeGrice IJ, Edgar SG, Loiselle DS. 3-Dimensional configuration of perimysial collagen fibres in rat cardiac muscle at resting and extended sarcomere lengths. The Journal of physiology. 1999;517 (Pt 3):831-7.
[18] Bruckner BA, Razeghi P, Stetson S, Thompson L, Lafuente J, Entman M, et al. Degree of cardiac fibrosis and hypertrophy at time of implantation predicts myocardial improvement during left ventricular assist device support. The Journal of heart and lung transplantation : the official publication of the International Society for Heart Transplantation. 2004;23:36-42.

Tables

Table S1. Content of selected sarcomeric proteins in non-failing and failing tissue

		cMyBP-C	cTnT	MLC-1	Actinin	MLC-2
Non-failing	Epi	1.17±0.18	1.63±0.47	1.24±0.14	1.07±0.17	1.22±0.22
	Mid	1.03±0.10	1.21±0.31	1.09±0.08	0.94±0.09	1.11±0.10
	Endo	1.11±0.10	1.25±0.37	1.16±0.11	0.92±0.07	1.22±0.22
Heart failure	Epi	1.03±0.07	1.10±0.29	1.12±0.10	1.06±0.07	1.15±0.11
	Mid	1.09±0.07	1.20±0.31	1.18±0.09	1.14±0.10	1.15±0.10
	Endo	0.88±0.10	1.01±0.34	0.95±0.14	0.99±0.30	1.01±0.15
Main statistical effects and interaction (p values)	Condition	0.388	0.616	0.589	0.439	0.702
	Region	0.448	0.655	0.395	0.452	0.725
	Condition *Region	0.231	0.455	0.243	0.537	0.639

Protein contents are expressed in arbitrary units and were calculated by normalizing to data obtained for each protein from a non-failing sub-epicardial sample that was loaded onto every gel as a control.

Table S2. Content of Myosin Heavy Chain (MHC) and Actin in non-failing and failing tissue

		MHC	Actin
Non-failing	Epi	0.79±0.08	0.71±0.10
	Mid	0.71±0.05	0.71±0.04
	Endo	0.78±0.06	0.71±0.04
Heart failure	Epi	0.74±0.03	0.66±0.02
	Mid	0.69±0.04	0.58±0.03
	Endo	0.71±0.07	0.62±0.07
Main statistical effects and interaction (p values)	Condition	0.345	0.092
	Region	0.534	0.764
	Condition*Region	0.920	0.772

Protein contents are expressed in arbitrary units and were calculated by normalizing to data obtained for each protein from a non-failing sub-epicardial sample that was loaded onto every gel as a control, and corrected for the initial weight of the original tissue sample.

Table S3. Phosphorylation of selected sarcomeric proteins in non-failing and failing tissue

		Phospho cMyBP-C	Phospho cTnT	Phospho cTnI	Phospho MLC-1	PSer273 cMyBP-C	PSer282 cMyBP-C
Non-failing	Epi	1.03±0.09	1.24±0.33	1.13±0.06	1.02±0.14	1.38±0.28	1.01±0.17
	Mid	1.05±0.1	1.59±0.30	1.38±0.24	1.26±0.18	1.39±0.35	1.01±0.14
	Endo	0.95±0.1	1.77±0.47	1.14±0.20	1.17±.0.11	1.38±0.35	1.01±0.21
Heart failure	Epi	0.79±0.05	1.91±0.46	1.40±0.32	1.34±0.19	1.31±0.27	0.97±0.08
	Mid	0.77±0.06	1.68±0.39	1.22±0.25	1.34±0.26	1.35±0.27	0.94±0.07
	Endo	0.86±0.16	2.16±0.49	0.89±17§	1.52±0.24	1.03±0.16	0.97±0.08
Main statistical effects and interaction (p values)	Condition	0.094	0.530	0.893	0.367	0.685	0.760
	Region	0.999	0.237	***0.041***	0.345	0.406	0.960
	Condition * Region	0.554	0.484	0.076	0.457	0.428	0.900

Phosphorylation levels are expressed in arbitrary units and were calculated by normalizing to data obtained for each protein from a non-failing sub-epicardial sample that was loaded onto every gel as a control.

Different from the sub-epicardial region of the same condition: § $p<0.05$.

Table S4. Statistically significant linear relationships between functional and biochemical data.

Biochemical variable	Functional parameter	r	p value
cTnI	Maximum force	0.291	***0.045***
Phospho MLC-1	V_{max}	-0.287	***0.048***
PSer273 cMyBP-C	V_{max}	0.396	***0.023***
PSer282 cMyBP-C	V_{max}	0.533	***0.001***
PSer23/24-cTnI	Passive stiffness	0.390	***0.025***
PSer23/24-cTnI	Passive force	0.467	***0.006***

Table S5. Functional contractile properties in non ischemic and ischemic tissue

		Maximum Power ($\mu W\ mg^{-1}$)	Maximum Force ($kN\ m^{-2}$)	Maximum Velocity ($mL\ s^{-1}$)	pCa_{50}
Non ischemic	Epi	0.37±0.04	9.79±1.10	1.05±0.07	5.68±0.02
	Mid	0.34±0.03	7.69±0.68	1.09±0.09	5.70±0.02
	Endo	0.31±0.02	9.33±1.09	0.93±0.05	5.65±0.05
Ischemic	Epi	0.43±0.03	12.41±0.83	1.00±0.05	5.69±0.03
	Mid	0.40±0.04	9.90±0.63	1.01±0.07	5.76±0.05
	Endo	0.36±0.05	9.38±1.09 §	1.06±0.09	5.72±0.04
Main statistical effects and interaction (p values)	Condition	0.348	0.228	0.999	0.535
	Region	***0.045***	***0.007***	0.773	0.140
	Condition *Region	0.845	0.145	0.334	0.286

Different from the sub-epicardial region of the same condition: § $p<0.05$.

Table S6. Content of selected sarcomeric proteins in non ischemic and ischemic tissue

		cMyBP-C	cTnT	MLC-1	Actinin	MLC-2
Non ischemic	Epi	0.88±0.08	1.09±0.52	0.91±0.10	0.95±0.10	0.96±0.10
	Mid	1.1±0.33	1.26±0.58	1.20±0.13	1.22±0.21	1.21±0.18
	Endo	1.00±0.13	1.22±0.57	0.98±.0.16	1.08±0.12	1.12±0.21
Ischemic	Epi	1.19±0.08	1.11±0.36	1.33±0.10	1.17±0.08	1.33±0.16
	Mid	1.08±0.05	1.68±0.39	1.17±0.14	1.05±0.03	1.10±0.12
	Endo	0.76±0.15 §	1.00±0.43	0.91±0.24 §	0.89±0.15	0.90±0.24
Main statistical effects and interaction (p values)	Condition	0.904	0.853	0.564	0.732	0.964
	Region	0.084	0.937	0.126	0.402	0.496
	Condition *Region	***0.025***	0.932	0.084	0.146	0.096

Protein contents are expressed in arbitrary units and were calculated by normalizing to data obtained for each protein from a non-failing sub-epicardial sample that was loaded onto every gel as a control. Different from the sub-epicardial region of the same condition: § $p<0.05$.

Table S7. Content of Myosin Heavy Chain (MHC) and Actin in non ischemic and ischemic tissue

		MHC	Actin
Non ischemic	Epi	0.70±0.04	0.64±0.04
	Mid	0.75±0.05	0.61±0.04
	Endo	0.81±0.04	0.66±0.05
Ischemic	Epi	0.78±0.02	0.68±0.02
	Mid	0.63±0.05	0.54±0.03
	Endo	061±0.13 †	0.58±0.14
Main statistical effects and interaction (p values)	Condition	0.217	0.608
	Region	0.733	0.515
	Condition*Region	0.124	0.574

Protein contents are expressed in arbitrary units and were calculated by normalizing to data obtained for each protein from a non-failing sub-epicardial sample that was loaded onto every gel as a control, and corrected for the initial weight of the original tissue sample. Effect of ischemic status on region: † $p<0.05$.

Table S8. Phosphorylation of selected sarcomeric proteins and residues in non ischemic and ischemic tissue

		Phospho cMyBP-C	Phospho cTnT	Phospho cTnI	Phospho MLC-1	PSer273 cMyBP-C	PSer282 cMyBP-C
Non ischemic	Epi	0.75±0.10	2.50±0.89	1.05±0.20	0.91±0.10	0.94±0.28	0.88±0.10
	Mid	0.84±0.07	1.93±0.64	0.97±0.29	1.20±0.13	1.25±0.44	0.91±0.11
	Endo	0.73±0.10	1.82±0.47	0.64±0.12	0.98±.0.16	0.80±0.17	0.88±0.10
Ischemic	Epi	0.83±0.03	1.70±0.45	1.18±0.60	1.33±0.10	1.80±0.49	1.09±0.11
	Mid	0.70±0.11	1.43±0.50	1.47±0.42	1.17±0.14	1.49±0.35	0.99±0.10
	Endo	0.10±0.32	2.50±0.89	1.15±0.30§	0.91±0.24 §	1.35±0.21	1.10±0.09 ‡
Main statistical effects and interaction (p values)	Condition	0.678	0.921	0.263	0.564	0.240	0.279
	Region	0.749	0.370	***0.01***	0.126	0.187	0.302
	Condition *Region	0.337	0.168	0.727	0.084	0.247	***0.043***

Phosphorylation levels are expressed in arbitrary units and were calculated by normalizing to data obtained for each protein from a non-failing sub-epicardial sample that was loaded onto every gel as a control

Different from the mid-myocardial region of the same condition: ‡ $p<0.05$. Different from the sub-epicardial region of the same condition: § $p<0.05$.

Table S9. Functional contractile properties in non-failing and ischemic tissue

		Maximum Power ($\mu W\ mg^{-1}$)	Maximum Force ($kN\ m^{-2}$)	pCa_{50}
Non-failing	Epi	0.46±0.03	10.96±0.74	5.619±0.01
	Mid	0.59±0.06§	14.30±1.33§	5.67±0.02
	Endo	0.46±0.04‡	11.47±0.86‡	5.69±0.02§
Ischemic	Epi	0.43±0.03	12.41±0.83	5.69±0.03
	Mid	0.40±0.04†	9.90±0.63†	5.76±0.05§
	Endo	0.36±0.05	9.38±1.09§	5.72±0.04
Main statistical effects and interaction (p values)	Condition	0.080	0.230	0.251
	Region	0.057	0.110	***0.001***
	Condition *Region	0.132	***0.004***	0.366

Effect of ischemic status on region: † $p<0.05$. Different from the sub-epicardial region of the same condition: § $p<0.05$. Different from the mid-myocardial region of the same condition: ‡ $p<0.05$.

Table S10. Functional contractile properties in non-failing and non ischemic tissue

		Maximum Power ($\mu W\ mg^{-1}$)	Maximum Force ($kN\ m^{-2}$)	pCa_{50}
Non-failing	Epi	0.46±0.03	10.96±0.74	5.619±0.01
	Mid	0.59±0.06§	14.30±1.33§	5.67±0.02
	Endo	0.46±0.04‡	11.47±0.86‡	5.69±0.02§
Non ischemic	Epi	0.37±0.04	9.79±1.10	5.68±0.02
	Mid	0.34±0.03†	7.69±0.68†	5.70±0.02
	Endo	0.31±0.02†	9.33±1.09	5.65±0.05
Main statistical effects and interaction (p values)	Condition	***0.009***	***0.040***	0.717
	Region	0.117	0.704	0.096
	Condition *Region	0.091	***0.004***	***0.004***

Effect of non ischemic status on region: † $p<0.05$. Different from the sub-epicardial region of the same condition: § $p<0.05$. Different from the mid-myocardial region of the same condition: ‡ $p<0.05$.

Figures

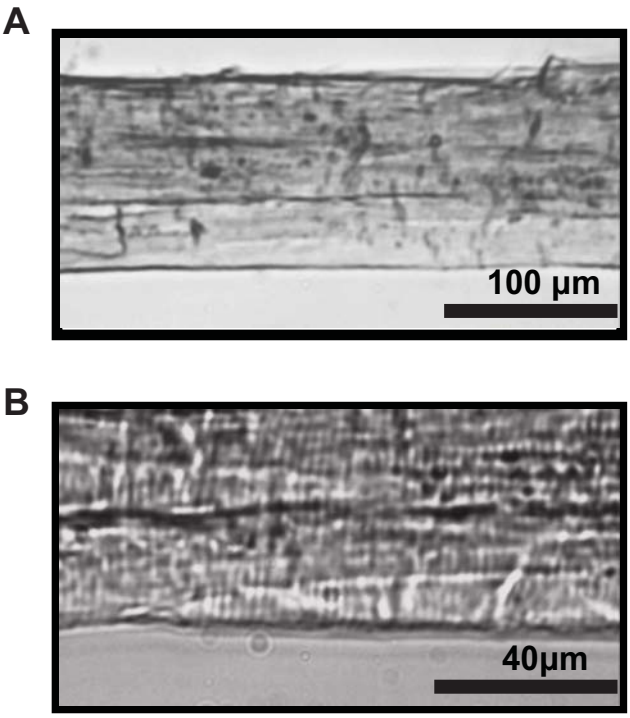

Figure S1. Experimental preparations.

Low (panel A) and high (panel B) magnification views of the central section of a representative myocardial preparation immersed in a solution with a pCa value of 9.0.

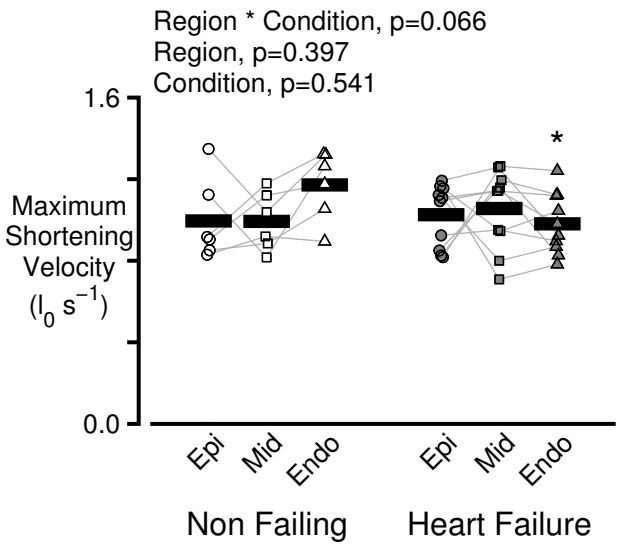

Figure S2. Maximum shortening velocity does not depend on heart failure status or transmural region.

Symbols show the mean of the maximum shortening velocities measured from 2 or 3 preparations from each region for each heart. In this figure, and in all similar panels, thin lines join data points from the same heart. Thick bars show the mean data for the region. The text above the plot shows p values for the main statistical effects. Significant differences between regions, tested separately for non-failing and failing hearts, are listed in the inset box. Significant differences due to heart failure, tested separately for each region, are indicated by asterisks (* $p<0.05$, ** $p<0.01$, *** $p<0.001$).

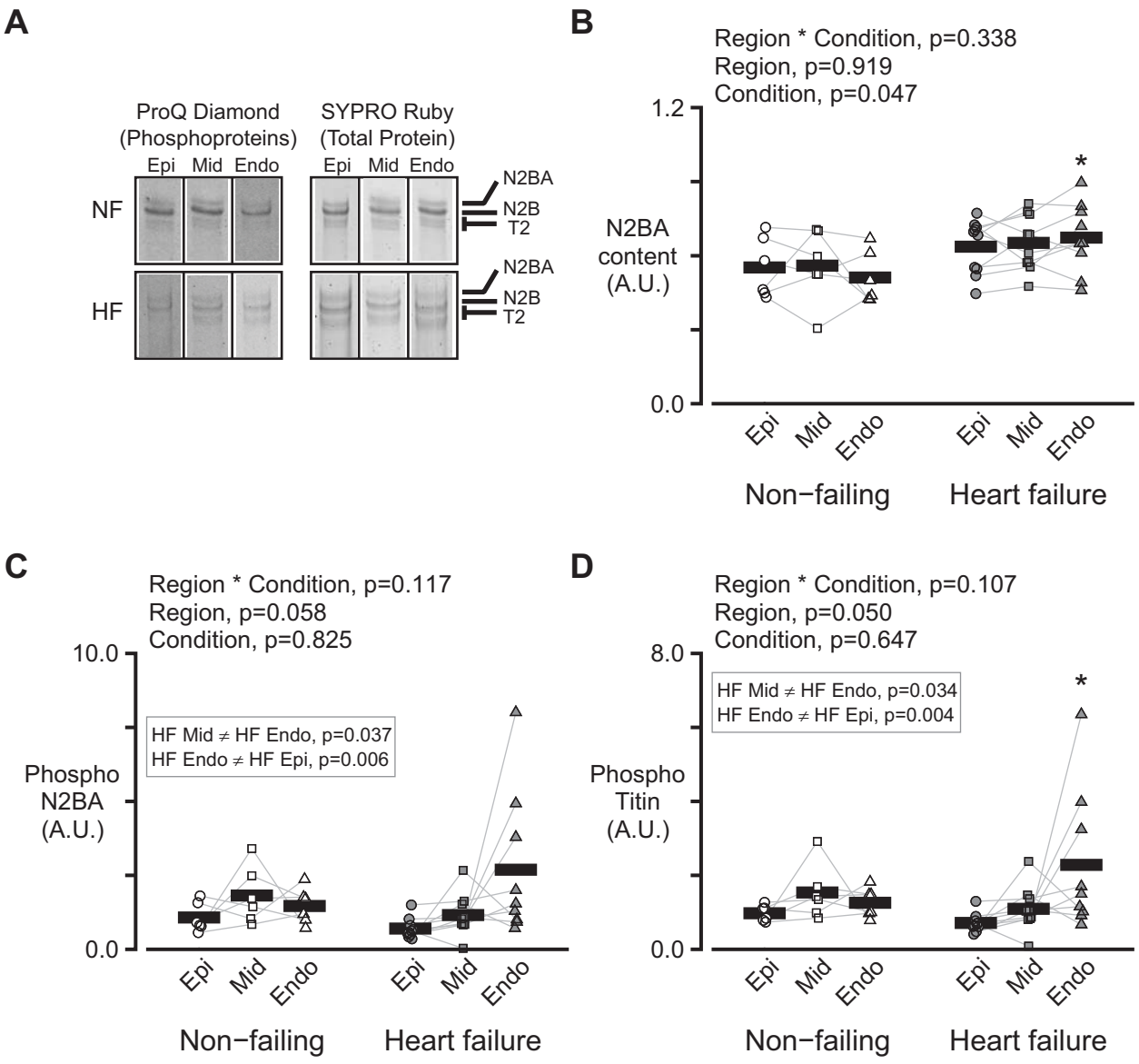

Figure S3. The relative content of the N2BA isoform of titin is increased in heart failure.

A) Titin gels stained with Pro-Q Diamond (left) and SYPRO Ruby (right). The figure shows lanes collated from several gels. The Pro-Q Diamond stain is sensitive to phosphoproteins while SYPRO Ruby indicates total protein content. B) Symbols show the relative content of the N2BA isoform for each region for each heart. A.U. stands for arbitrary units. C) As for panel B but showing the relative content of phosphorylated

N2BA protein. D) As for panel B but showing the relative content of phosphorylated total titin.

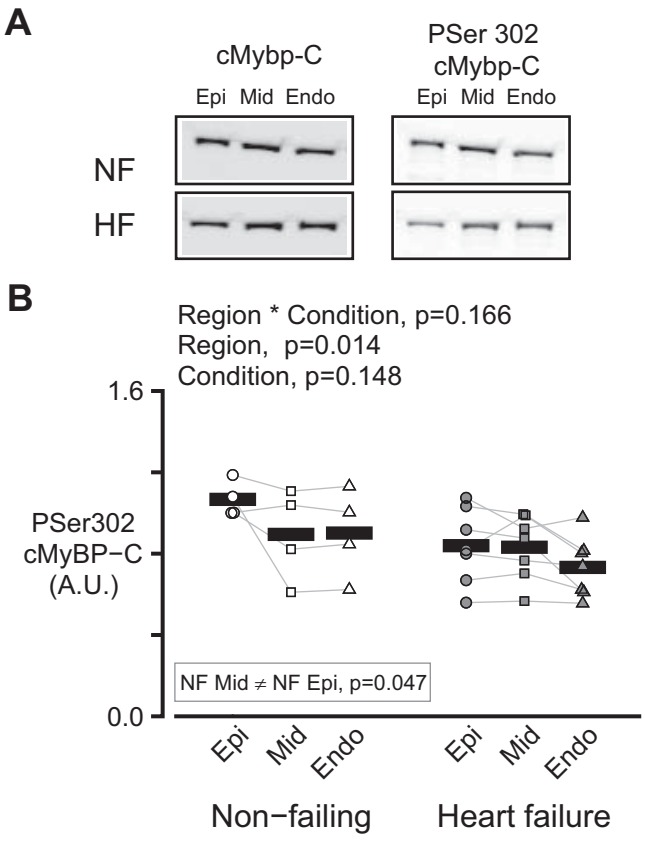

Figure S4. PSer302 cMyBP-C depends on transmural region.

A) Representative immunoblots showing total cMyBP-C and PSer302 cMyBP-C for non-failing and failing hearts. B) Symbols show the mean PSer302 cMyBP-C measured for each region for each heart. A.U. stands for arbitrary units.

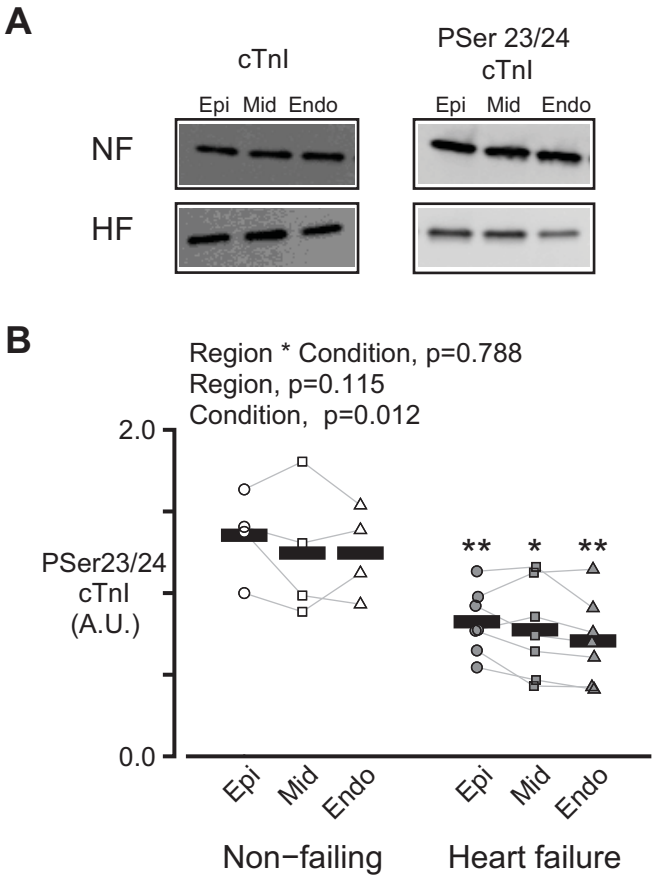

Figure S5. PSer23/24 cTnI is reduced in heart failure.

A) Representative immunoblots showing total cTnI and PSer23/24 cTnI for non-failing and failing hearts. B) Symbols show the mean PSer23/24 cTnI measured for each region for each heart. A.U. stands for arbitrary units.

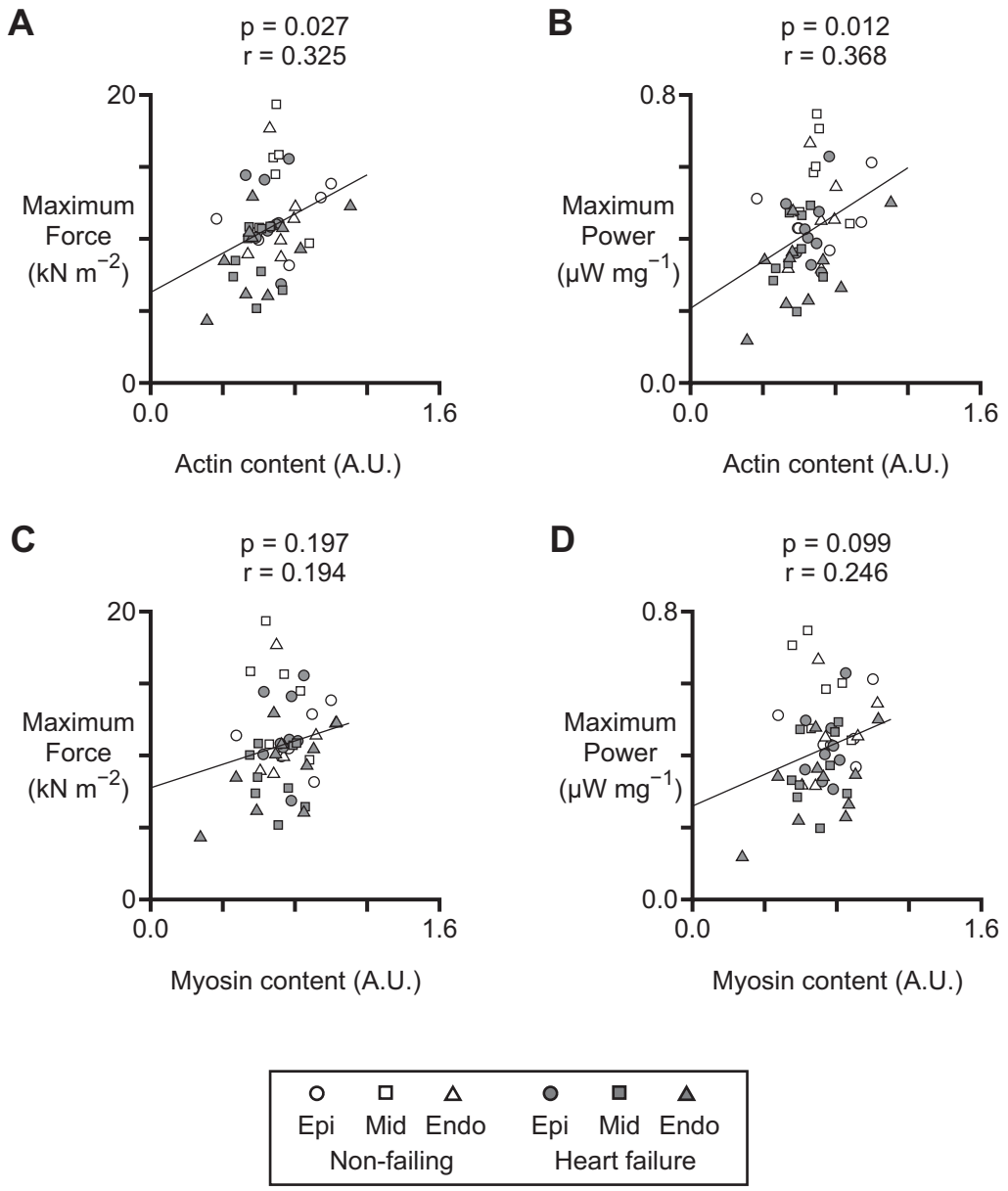

Figure S6. Contractile function is reduced with decrease in actin content.

A) Maximum Force and B) Maximum Power plotted against the actin content. C) Maximum Force and B) Maximum Power plotted against the myosin content. Protein content was determined by Lowry protein assays and corrected for initial weight of the tissue (Table S2 and gel electrophoresis Figure 5A). A.U. stands for arbitrary units. The

plots show the best-fit straight lines determined by linear regression and the corresponding p and r values.

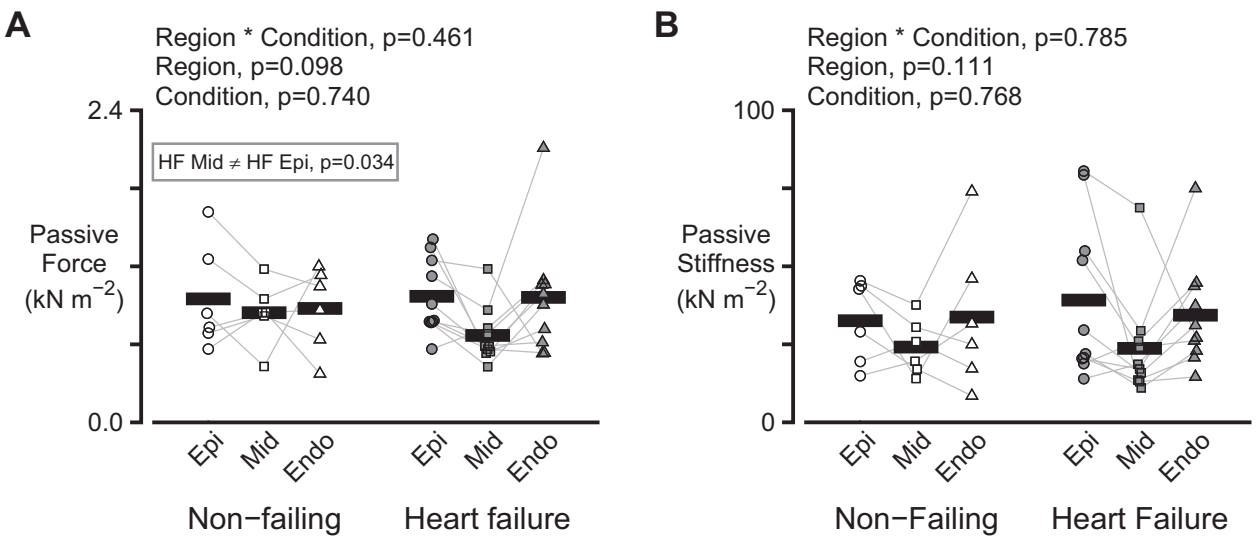

Figure S7. Passive force and passive stiffness do not depend on heart failure status.

Passive force (panel A) and passive stiffness (panel B) measured in pCa 9.0 solution. Stiffness values are expressed as Young's Moduli and were calculated by fitting regression lines to the force responses measured during 4% length changes imposed at a speed of 0.12 l_0 s^{-1}. In both plots, symbols show the mean data value measured from 2 or 3 preparations from each region for each heart.

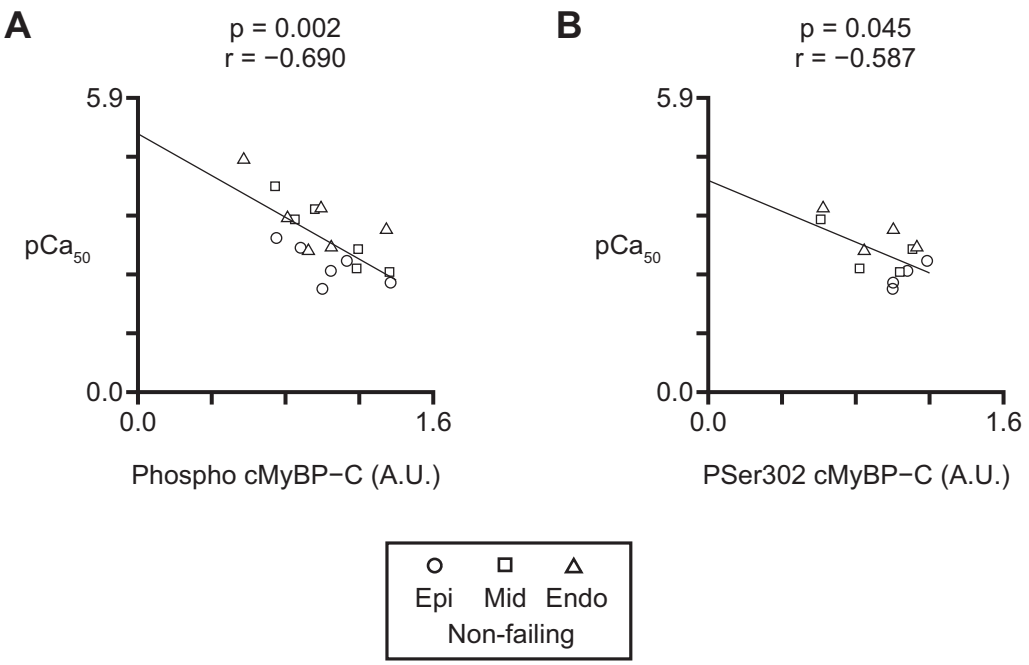

Figure S8. Ca^{2+} sensitivity of non-failing samples depended on the phosphorylation of cMyBP-C.

Ca^{2+} sensitivity of non-failing samples correlated significantly with A) total phosphorylation of cMyBP-C and B) site-specific phosphorylation of cMyBP-C at Ser302. A.U. stands for arbitrary units. The plots show the best-fit straight lines determined by linear regression and the corresponding p and r values.

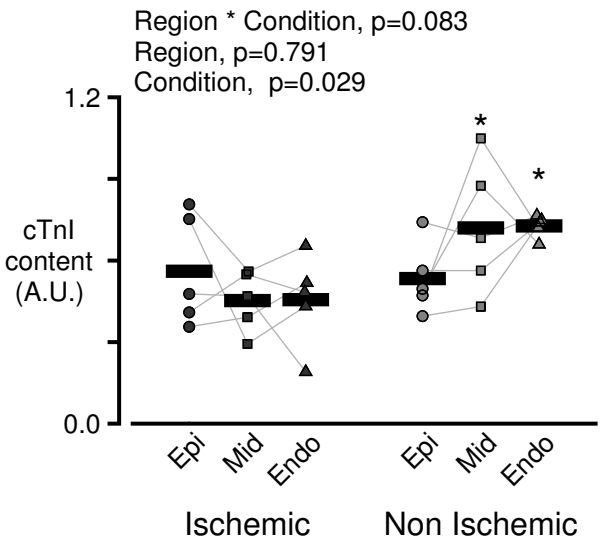

Figure S9. cTnI content is reduced in ischemic heart failure.

Symbols show the mean cTnI content measured for each region for failing hearts using SYPRO Ruby stain (indicates total protein) with ischemic disease (left) and non ischemic disease (right).

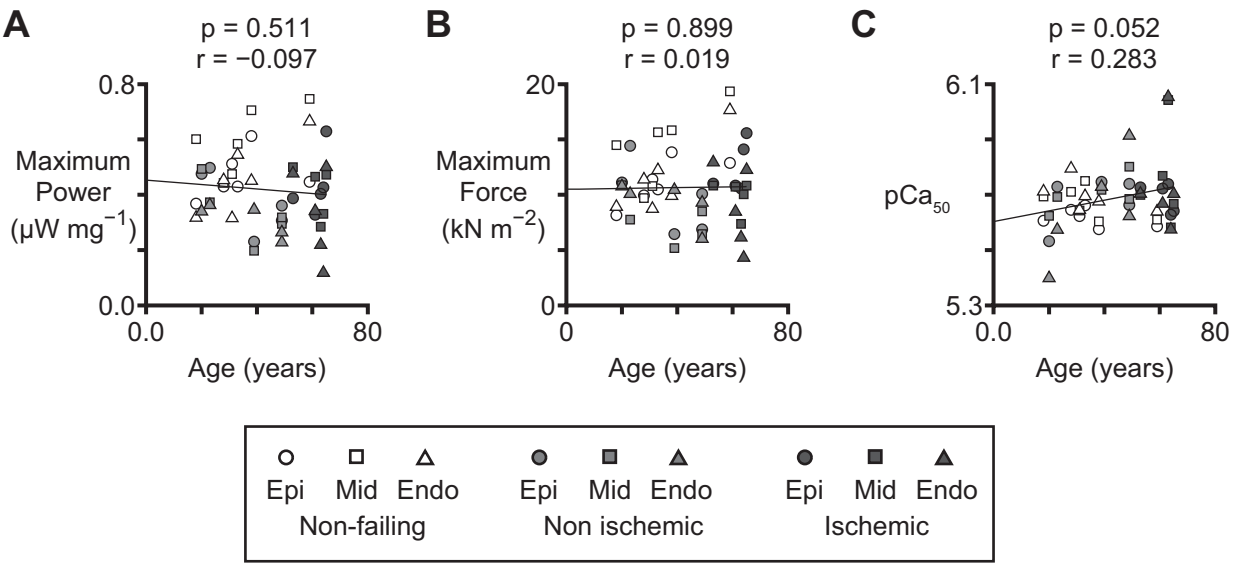

Figure S10. No statistically significant relationships between contractile properties and age.

Each panel shows the relationship between a selected functional parameter and Age. The y coordinate of each symbol indicates the mean value of a functional parameter measured from 2 or 3 preparations from each region for each heart. The x coordinate of each symbol shows the age of the individual patient/donor. The plots also show the best-fit straight lines determined by linear regression and the corresponding p and r values.

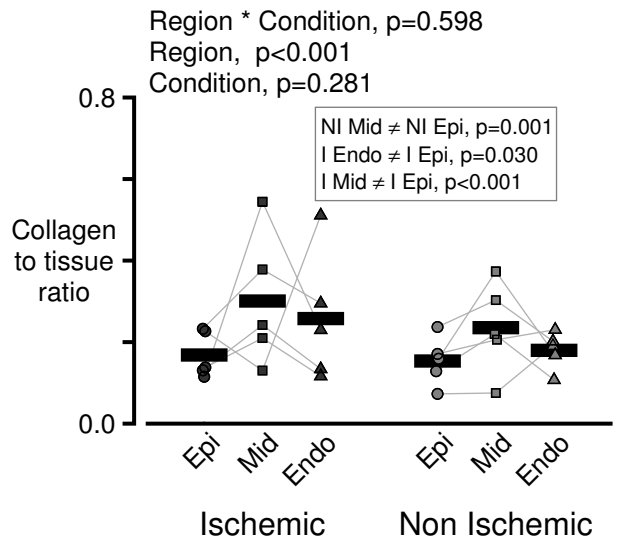

Figure S11. Collagen content is increased in the mid-myocardium of patients with ischemic and non ischemic disease.

Symbols show the mean collagen to tissue ratio measured for each region for failing hearts with ischemic disease (I, left) and non ischemic disease (NI, right).

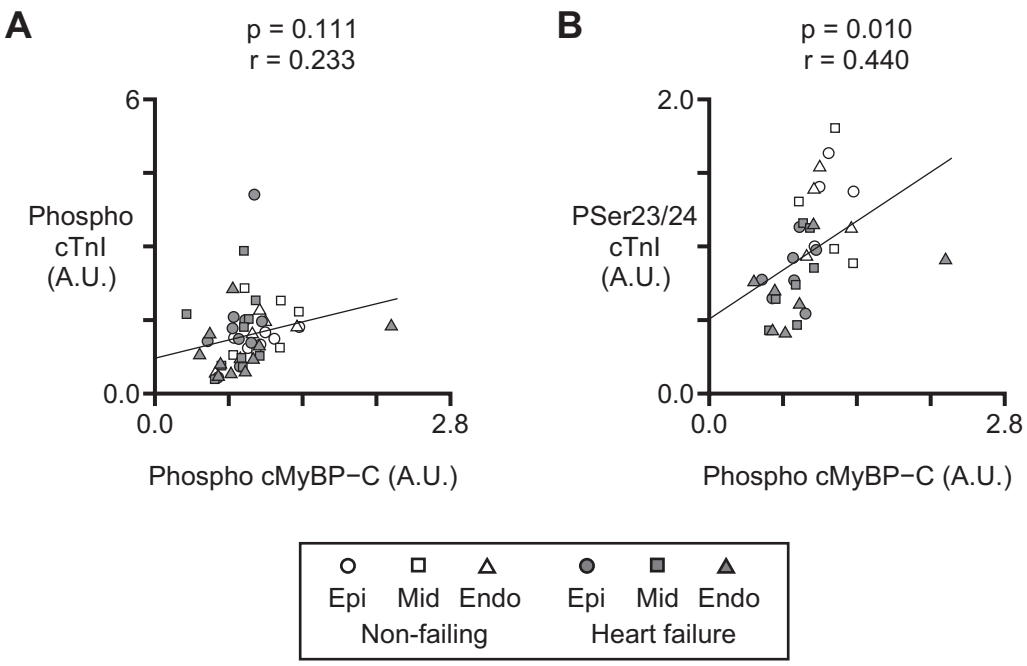

Figure S12. Site-specific phosphorylation of cTnI at Ser23/24 correlated with phosphorylation of cMyBP-C.

A) Total phosphorylation and B) site-specific phosphorylation of cTnI at Ser23/24 correlations with total phosphorylation of cMyBP-C. A.U. stands for arbitrary units. The plots show the best-fit straight lines determined by linear regression and the corresponding p and r values.

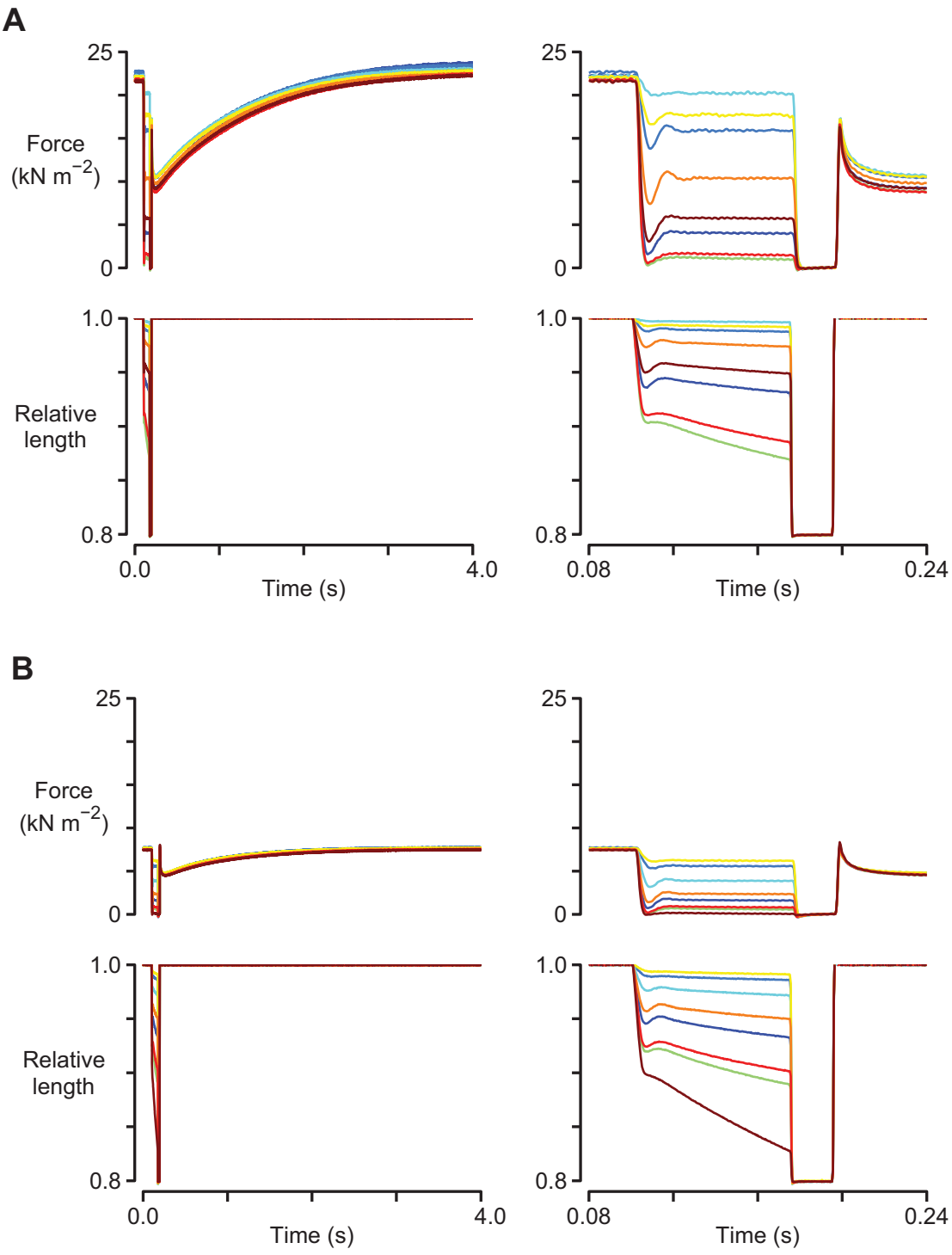

Figure S13. Mechanical records.

Superposed force and length records obtained during force-velocity experiments performed with a representative preparation isolated from the mid-myocardium of A) a non-failing heart and B) a failing heart. The left hand shows the x-axis time-scale for the complete experiments. The right hand side shows the expanded x-axis time-scale for the same experiments.